Vanishing Point and Gabor Feature based Multi-Resolution On-Road Vehicle Detection

Hong Cheng[1], Nanning Zheng[1], Chong Sun[1], and Huub van de Wetering[1,2]

[1] Institute of Artificial Intelligence and Robotics,Xi'an Jiaotong University,China,
hcheng@mail.xjtu.edu.cn nnzheng@mail.xjtu.edu.cn
[2] Technische Universiteit Eindhoven, Netherlands,

Abstract. Robust and reliable vehicle detection is a challenging task under the conditions of variable size and distance, various weather and illumination, cluttered background, the relative motion between the host vehicle and background. In this paper we investigate real-time vehicle detection using machine vision for active safety in vehicle applications. The conventional search method of vehicle detection is a full search one using image pyramid,which processes the image patches in same way and costs same computing time, even for no vehicle region according to prior knowledge.
Our vehicle detection approach includes two basic phases. In the hypothesis generation phase, we determine the Regions of Interest (ROI) in an image according to lane vanishing points; furthermore, near, middle, and far ROIs, each with a different resolution, are extracted from the image. From the analysis of horizontal and vertical edges in the image, vehicle hypothesis lists are generated for each ROI. Finally, a hypothesis list for the whole image is obtained by combining these three lists. In the hypothesis validation phase, we propose a vehicle validation approach using Support Vector Machine (SVM) and Gabor feature.The experimental results show that the average right detection rate reach 90% and the average execution time is 30ms using a Pentium(R)4 CPU 2.4GHz.

1 Introduction

Statistics shows that about 60% of the rear-end crash accidents can be avoided if the driver has additional warning time. According to the Ministry of Public Safety P.R.China, there were 567,753 reported road traffic accidents in 2004, among those about 80% of the severe police-reported traffic accidents are vehicle-vehicle crashes. Clearly, vehicle detection is an important research area of intelligent transportation systems [1] [2]. It is being used in, among others, adaptive cruise control (ACC), driver assistance systems, etc. However, robust detection of vehicle in real-life traffic scenes is challenging.

This paper introduces a hypothesis-validation structure which consists of the three steps described below. Firstly, ROI determination using the vanishing point of lane markings. Secondly, vehicle hypothesis generation for each ROI using horizontal and vertical edge detection. Finally, hypothesis validation using Gabor features of 9 sub-windows and SVM classifiers.

2 Related Work

Hypotheses are generated using some simple features, such as, color, horizontal\ vertical edges, symmetry[2][3], motion, and stereo visual cue. Zehang Sun proposed a multi-scale hypothesis method, in which the original image was downsampled. His vehicle hypotheses were generated by combining the horizontal and vertical edges of these three levels and this multi-scale method greatly reduced the random noise. This approach can generate multiple-hypothesis objects, but a near vehicle may prevent a far vehicle from being detected. As a result, it fails to generate the corresponding hypothesis of the far vehicle reducing the vehicle detection rate.

Vehicle symmetry is an important cue in vehicle detection and tracking. Inspired by the voting of Hough Transform, Yue Du proposed a vehicle following approach by finding the symmetry axis of a vehicle [3]; however, his approach has several limitations, such as large computing burden, and it only generates one object hypothesis using the best symmetry. A. Broggi introduced a multi-resolution vehicle detection approach, and proposed to divide the image into three fixed ROIs: one near the host car, one far from the host car, and one in the middle[2]. This approach overcomes the limit that it only can detect a single vehicle in the predefined region of the image but it needs to compute symmetry axis making it not real-time.

Accordingly, in this paper we detect vehicles only in ROIs allowing us to make a real-time implementation. The ROI approach largely prevents a near car from hiding a far car. All the hypotheses are generated in these regions. The positions of vehicles are validated by SVM classifiers and Gabor features.

3 Generating Candidate ROIs

Inspired by A.Broggio [2], we extract three ROIs, a near one, one in the middle, and far one, from the 640×480 image. But his approach uses fixed regions at the cost of flexibility. In this paper, ROIs are extracted using lane markings. In a structured lane, we detect the vanishing point using the lane edges. For the consideration of real-time processing, we use a simple vanishing point detector rather than a complex one. Discontinuity and noise related problems can be solved by combining, for instance, 10 subsequent images. In edge detection is done on combined images consisting of ten overlapping subsequent images, and the equations of two lanes are deduced from a voting procedures like hough transform by analyzing horizontal and vertical edges. Four random points $P_{di},\ d = l\ or\ r;\ i = 1,\ \cdots,\ 4$, are selected on each lane line, and each tangent direction of two points between the closed 3 points

$$\{P_{di}, P_{dj}\}; d = r\ or\ l; i, j \in \{0, 1, 2, 3\}; i < j; |j - i| \leq 2 \tag{1}$$

are obtained by

$$\theta_{dij} = \overrightarrow{P_{di}P_{dj}}$$

The tangent directions of two lane lines are calculated using average value of the above tangent angles, described by

$$\bar{\theta}_d = \frac{\theta_{d01} + \theta_{d02} + \theta_{d12} + \theta_{d13} + \theta_{d23}}{5}, d = r \ or \ l \tag{2}$$

Combining the average coordinates of 4 interesting points $\bar{P}_d = \frac{1}{4}\sum_{i=0}^{3} P_{di}$with the average tangent angles $\bar{\theta}_d$, we can get the equations of two lane lines. The intersection point of the two lines is the approximation of vanishing point, shown in Fig.1.

Next we consider how to extract ROI from the original image. For the consideration of vehicle height and the camera parameters, the top boundaries of all the ROIs are 10 pixels higher than the vertical coordinates of the vanishing point. From the analysis of the camera parameters and image resolution, the heights of the near, middle, and far ROIs are 160, 60, and 30 pixels, respectively. The left and right boundaries of the near ROI are those of the image. The distance between the left boundary of the middle ROI and that of the image is just one-third of the distance between vanishing point and the left boundary of the image, and the right one of middle ROI is determined similarly. The distance between the left boundary of the far ROI and that of image is two-thirds of the distance between vanishing point and the left boundary of image, as well as the distance between the right boundary of the far ROI and that of image.Fig. 1(b) shows the results of each ROI.

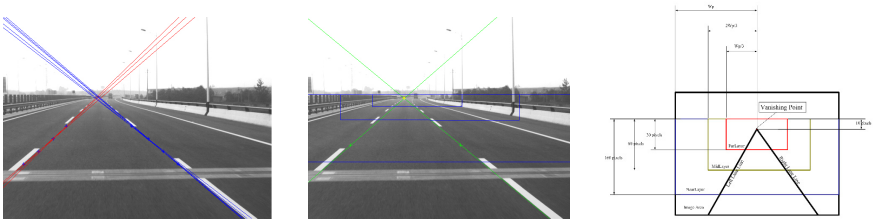

(a) Linking Lines between Interesting Points (b) Division of ROI (c) Lane ROI Generation

Fig. 1: Vanishing Point and ROI Generation

4 Multi-Resolution Vehicle Hypothesis

For traditional approaches, edges of small object cover those of a large one. The results of a global histogram of horizontal and vertical edges show the edge histogram without a peak for the small vehicle. Based on the preceding candidate regions, the histogram of a ROI shows a peak for a small object.The analysis of

the peaks and valleys of an edge histogram results in several rectangles and each one represents a vehicle hypothesis. We use prior knowledge to eliminate some hypotheses. The minimum width of a vehicle can be set for each ROI. If the width of a hypothesis is smaller than this width, the hypothesis will be eliminated. Additionally, the aspect ratio (width/height) of vehicles is in a certain range, we assume in the range $[0.67, 2.2]$; rectangles with other ratios are eliminated. Since the histogram is made by extracting edges from the ROIs and other objects, like power cables and traffic signs above the road are not in the ROIs, they do not disturb the edge histogram, reducing the false positive rate. The coordinates of all hypothesis objects will be translated into the coordinates of the original image, and then the hypotheses of different ROIs may be overlapping. According to the distance between two rectangles, $d(r_1, r_2)$, we can judge if the two rectangles ought to be incorporated into one. Equ. 3 defines the distance between rectangle r_1 and r_2, and here (x_{ij}, y_{ij}) is the coordinates of the j-th vertex of i-th rectangle, i=1,2, j=1,2,3,4. Through the above process,we finish the generation of vehicle hypotheses.

$$d(r_1, r_2) = \| r_1 - r_2 \|_2, \quad r_i = (x_{i1}, y_{i1}, x_{i2}, y_{i2}, x_{i3}, y_{i3}, x_{i4}, y_{i4}), i = 1, 2 \tag{3}$$

5 Vehicle Validation Using Gabor Feature and SVM

5.1 Vehicle Representation

We first introduce some necessary definitions for Gabor filters and basic concepts for vehicle representation. The 2D Gabor function can be defined as follows

$$G_{\{f,\varphi,\sigma_u,\sigma_v\}}(u, v) = \frac{1}{2\pi\sigma_u\sigma_v} exp[-\frac{1}{2}(\frac{U^2}{\sigma_u^2} + \frac{V^2}{\sigma_v^2})] \cdot exp[2\pi j f U] \tag{4}$$

Where

$$\begin{cases} U = (u, v) \cdot (cos\varphi, sin\varphi \\ V = (-u, v)(sin\varphi, cos\varphi) \end{cases}$$

And f means the normalized spatial frequency of a complex sinusoidal signal modulating Gaussian function, φ is the direction of a Gabor filter, σ_u and σ_v are the scale parameters of filter. Therefore, $\{f, \varphi, \sigma_u, \sigma_v\}$ can represent the parameters of a Gabor filter. Actually, a Gabor filter is a bandpass filter, and the first step of vehicle detection is to select the Gabor filters strongly responding to the detected object.

We select the filter parameters with the strongest response for certain sub-window including a vehicle part, and use SVM as a performance estimation classifier. The test image is divided into 9 overlapping sub-windows, and the statistical Gabor features from convolution between sub-window image patch and a Gabor filter, mean μ, standard deviation θ, and the skewness κ, represent the vehicle [6]. We optimize the SVM parameters for each of the nine sub-windows, and test the resulting nine classifiers for each sub-window using test examples, and record the average error rate. At last, for each sub-window, the

Table 1: Selection of the Optimized Gabor Features

(1).To give the test error rate for m'th sub-window by $(x_i, y_i)_{i=0}^{N}$,where x_i is the parameter vector,y_i is the error rate;$Y_0 = \{y_0, y_1, \ldots, y_N\}$. $P_0 = \{\}$;
(2).To select the optimized filters
For t=0,1,2,3
Here:$index = argmin \parallel Y_t \parallel_\infty$
$Y_t = Y_t - \{y_{index}\}$
if $\parallel x_{index} - x_j \parallel > \epsilon, x_j \in P_t$
then $P_t = P_t + \{x_{max_t}\}$
else
goto Here
(3). To get the best Gabor filter bank for m'th sub-window.

4 Gabor filters with the minimum average error rate are combined into a filter bank for extracting a feature vector (See Table 1).

Then the 9 sub-windows with 4 Gabor filters each make a feature vector of size 108,

$$[\mu_{11},\ \theta_{11},\ \kappa_{11},\ \mu_{12},\ \theta_{12},\ \kappa_{12},\ \cdots,\ \mu_{93},\ \theta_{93},\ \kappa_{93},\ \mu_{94},\ \theta_{94},\ \kappa_{94}]$$

Where $\mu_{ij},\ \theta_{ij},\ \kappa_{ij}$, are the mean, standard deviation, and skewness; i is the number of a sub-window, j is the number of a filter.

6 Results and Discussions

6.1 Test Results and Discussions

For training the SVM classifiers, we selected 500 images from our vehicle database which was collected in Xi'an in 2005. They contain 1020 positive examples and 1020 negative examples. In testing the classifier, we get above 90% average right detection rate using 500 negative and positive examples independent of the training examples, and the missing and error detection rate is below 10%.

We tested our vehicle detector on the collected video using the Springrobot platform.Fig. 2 show the results of our vehicle detector under general and hard conditions. We proposed an approach for vehicle classification and detection with good time performance using vanishing points and ROIs while achieving high detection accuracy using Gabor feature. The method using the vanishing point to define ROIs, eliminates the disturbing effects of some non-vehicle objects improving both the detection rate and the robustness of this approach. The detection speed of our vehicle detector is approximately 20 frames/second on a Pentium(R) 4 CPU 2.4GHz both for general and hard conditions.

Extension of this approach to unstructured roads needs to be investigated. Further research work will focus on these problems.

Fig. 2: Vehicle Detection Result Under the General and Hard Conditions

Acknowledgements

The work is supported by the National Natural Science Foundation of China (60021302) and OMRON company from Japan for their support and assistance.

References

1. Zheng, N. N. , Tang, S. , Cheng, H. , Li, Q. , Lai, G. , Wang, F. Y.: Toward Intelligent Driver-Assistance and Safety Warning System, IEEE Intelligent Systems 19(2) (2004) 8 - 11
2. Broggi, A. , Cerri , P. , Antonello, P. C : Multi-Resolution Vehicle Detection Using Artificial Vision. In: IEEE International Symposium on Intelligent Vehicle. (2004) 310 - 314
3. Du, Y., Papanikolopoulos, N.P.: Real-Time Vehicle Following Through a Novel Symmetry-Based Approach. In: IEEE International Conference on Robotics and Automation, Vol. 4. (1997) 3160 - 3165
4. Rasmussen, C. , : Grouping Dominant Orientations for Ill-Structured Road Following. In: Proceedings of the 2004 IEEE International Conference on Computer Vision and Pattern Recognition, Vol. 1. (2004) 470 - 477
5. Manjunath, B. and Ma W. : Texture Features for Browsing and Retrieval of Image Data, IEEE Transactions on Pattern Analysis and Machine Intelligence 18(8) (1996) 837 - 842
6. Sun, Z. H. , Miller R. , Bebis, G. , and DiMeo D. : On-road Vehicle Detection Using Evolutionary Gabor Filter Optimization, IEEE Transactions on Intelligent Transportation Systems 6(2) (2005) 125 - 137